Scientific Research Publishing

Advances in Nanoparticles, 2023, 12, 68-79
https://www.scirp.org/journal/anp
ISSN Online: 2169-0529
ISSN Print: 2169-0510

Performance of Rhodamine-Sensitized Solar Cells Fabricated with Silver Nanoparticles

Bandana Ranamagar, Isaac Abiye, Himsheela Karki, Yucheng Lan, Fasil Abebe*

Department of Chemistry, Morgan State University, Baltimore, MD, USA
Email: *Fasil.Abebe@morgan.edu

How to cite this paper: Ranamagar, B., Abiye, I., Karki, H., Lan, Y. and Abebe, F. (2023) Performance of Rhodamine-Sensitized Solar Cells Fabricated with Silver Nanoparticles. *Advances in Nanoparticles*, **12**, 68-79.
https://doi.org/10.4236/anp.2020.122006

Received: April 4, 2023
Accepted: May 27, 2023
Published: May 30, 2023

Abstract

A plasmonic effect of silver nanoparticles (AgNPs) in dye-sensitized solar cells (DSSCs) is studied. In this investigation, the efficiency of dye-sensitized solar cells has been remarkably increased by infusion of synthesized silver nanoparticles into the TiO_2 photoanode. Rhodaminederivative **RdS1** was synthesized by microwave-assisted condensation of hydrazide and 3-formylchromone. The synthesized silver nanoparticles were characterized with UV/Vis absorption spectroscopy and transmission electron microscopy. The interfacial charge transport phenomena of the dye-sensitized solar cell (DSSCs) are determined by electrochemical impedance spectroscopy and the corresponding efficiencies are calculated using current-voltage (I-V) curve. The solar cell photoanode with silver nanoparticles infused with **RdS1** in titanium dioxide had the highest solar-to-electric power efficiency at 0.17%.

Keywords

TiO_2, Silver Nanoparticles, Rhodamine, Optical, Dye-Sensitized Solar Cell

1. Introduction

Dye-sensitized solar cells (DSSCs) have received widespread application due to their low cost, lightweight, low toxicity, ease of fabrication, customizable design with flexibility, and good performance under diverse illumination [1] [2]. Many technological innovations have been developed to improve the efficiency and, at the same time, to reduce the cost of production ranging from interfacial modification [3] to material choices and engineering [4]. The number of studies focused on the large-scale production of DSSCs, and optimization has grown exponentially. A photosensitizing dye is used in DSSCs to convert solar energy into electrical energy. A typical DSSC consists of a dye-adhered nanocrystalline TiO_2

photoanode on a Fluorine-doped Tin Oxide (FTO) substrate, counter electrode, and an electrolyteiodide/triiodide (I^-/I_3^-) [5]. Distinct types of dye have been used to fabricate DSSCs with varying solar-to-electricity conversion efficiencies, and some among them are rhodamine dyes [6] [7]. The incorporation of plasmonic metal nanoparticles into the electrode of the dye-sensitized solar cells to boost the light absorption due to their localized surface plasmon effect has been very outstanding [8] [9]. When light interacts with the free electrons of the metal nanoparticles, surface plasmon resonance (SPR), a property of metal nanoparticles, is created. Thus, incorporating Silver Nanoparticles (AgNPs) increase light absorption in the photo-anode layer of dye-sensitized solar cells. Rhodamine is a reasonably priced broad band photosensitizer with good visible and near-infrared absorption spectra, and it has the essential characteristics needed to function as a photosensitizer. The long absorption and emission wavelengths, high fluorescence quantum yield, high extinction coefficient, and outstanding photostability of rhodamine dyes also make Rhodamine ideal for use in fluorescent sensor fabrication [10] [11].

In the present work, we report the synthesis of plasmonic silver nanoparticles and their application in TiO_2 photoanode for enhancing the performance of DSSCs. The performance of DSSCs with and without AgNPs were compared and there was found to be improved efficiency for DSSCs with silver nanoparticles.

2. Experimental Details

2.1. Materials and Methods

All the reagents and solvents were acquired from Sigma-Aldrich, including 3-formylchromone, Rhodamine-6G, hydrazine hydrate (85%), silver nitrate, sodium borohydride, acetic acid, ethanol, acetone, and iodide/triiodide electrolyte. Water-based colloidal graphite used in making the counter electrode was purchased from Electron Microscopy Sciences (EMS). The titanium dioxide (TiO_2) film was prepared with Titanium (IV) oxide, anatase (<25 nm) powder purchased from Sigma-Aldrich. The conducting fluorine-doped tin oxide (FTO) glass (50 mm × 50 mm × 2.2 mm) was obtained from Sigma-Aldrich.

The performance of the solar cell was evaluated using a 150 W fully reflective solar simulator with a standard illumination of air-mass 1.5 global (AM 1.5 G filter) having an irradiance of 100 mW/cm^2 (Sciencetech Inc, London, Ontario, Canada). An Interface1010E potentiostat/galvanostat/ZRA used for current, voltage, and impedance measurements were purchased from GAMRY Instruments (Warminster, PA, USA). The particle size and surface morphology of the synthesized-silver nanoparticles and silver-nanoparticle-infused titanium dioxide were examined with a JEOL transmission electron microscope with an accelerating voltage of 120 KV and a LaB6 electron gun (MA, USA). All absorption and fluorescence spectra were recorded using an Agilent Cary 60 UV/Vis absorption spectrometer and a Cary Eclipse fluorescence spectrophotometer, respectively.

2.2. Synthesis and Characterization of Silver Nanoparticles

Silver nanoparticles (AgNPs) were prepared following a previously reported method [12] using sodium borohydride ($NaBH_4$) to reduce silver nitrate ($AgNO_3$). Briefly, silver nanoparticles (1 mM) and sodium borohydride (2 mM) solutions were prepared in ice-chilled pure water. The two solutions were mixed slowly with constant stirring, and a yellowish color solution appeared. The mixture was cooled for 20 minutes in ice bath, where the ice bath is used to slow down the reaction and give better control over final particle size/shape. Silver ions were reduced and clustered to form monodispersed nanoparticles as a transparent solution in the aqueous medium. The silver nanoparticle was characterized by UV-V spectroscopy (Agilent Cary 60 UV/Vis's) and High Resolution-Transmission Electron Microscopy (120 KV JEOL).

2.3. Fabrication of the Dye-Sensitized Solar Cells

The titanium dioxide paste was prepared by mixing TiO_2 powder (1 g), ethylene glycol (1 mL), and glacial acetic acid (3 mL). Silver nanoparticle-based titanium dioxide paste was prepared by mixing TiO_2 powder (1 g), ethylene glycol (1 mL), and silver nanoparticle (3 mL) [13] [14] [15]. The anode was prepared by subsequently administering TiO_2 paste via the doctor-blade method, using a glass rod and adhesive tape to form a 2 × 2 cm rectangle, on the conductive surface of the FTO glass [16]. The FTO glass was air dried for 10 min and then annealed at 450˚C for 30 min. The annealed titanium dioxide was immersed in **RdS1** solution overnight. To prepare the cathode, colloidal graphite was applied to the conductive surface of the FTO glass and then dried at 80˚C for 10 min [17]. The components of the DSSC were assembled by fitting the TiO_2-coated FTO glass on top of the colloidal graphite-coated FTO glass, followed by the introduction of redox iodide/triiodide electrolyte solution. The electrolyte was dropped between the photoanode and counter electrode and allowed to spread down by capillary action. The systematic complete assembly of a plasmonic DSSC and energy diagram is shown in **Figure 1** (**Scheme 1**, **Scheme 2**).

2.4. Microwave-Assisted Synthesis of RdS1

Rhodamine hydrazide intermediate was synthesized according to Yang's method [18]. A mixture of rhodamine hydrazide intermediate (100 mg, 0.21 mmol), Chrome-3-carboxaldehyde (22 mg, 0.04 mmol) and 2 mL of ethanol was placed in a microwave vessel (**Scheme 1**). The resulting mixture was stirred and placed in a reactor. The reaction vessel was then run under pressure and irradiation at a specific temperature and time. After cooling, the reaction mixture was filtered and washed with cold ethanol. After drying, the solid product was isolated, and obtained, yield 80%. ^{1}H-NMR (d_6-DMSO), δ (ppm): 8.5 (s, 1H), 8.4 (s, 1H), 8.0 (m, 1H), 7.9 (m, 1H), 7.71 (m, 1H), 7.60 (m, 3H), 7.50 (m, 1H), 7.00 (d, 1H), 6.27 (s, 2H), 6.10 (s, 2H), 5.01 (s, 2H, -NH), 3.14 (t, 4H, NCH_2CH_3), 1.87 (s, 6H, $-CH_3$), 1.21 (t, 6H, NCH_2CH_3). ^{13}C-NMR (DMSO), δ (ppm): 165.23, 152.07, 151.33,

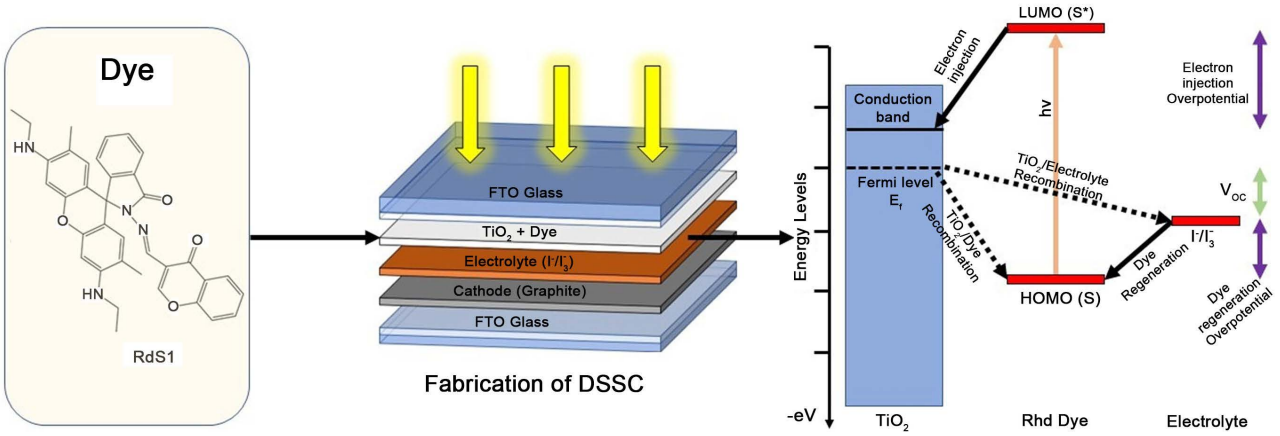

Figure 1. Schematic of a plasmonic DSSC.

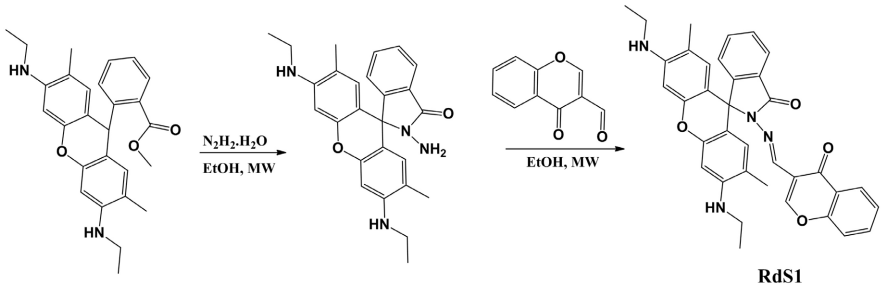

Scheme 1. Microwave-assisted synthesis of compound **RdS1**.

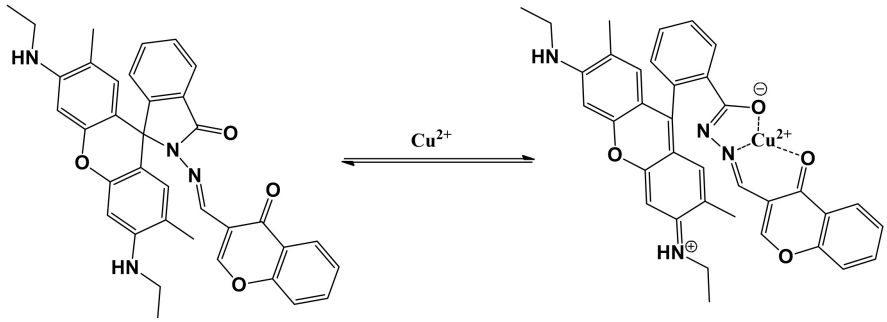

Scheme 2. Synthesis of complex **RdS1-Cu²⁺**.

147.35, 132.31, 129.48, 128.00, 127.01, 123.43, 122.13, 117.79, 104.99, 95.85, 64.96, 55.99, 37.45, 18.53, 17.06, 14.20. HRMS (MALDI): m/z Calcd for **S1** (M + 1): 585.2496; Found: 585.2504.

3. Results and Discussion

3.1. Optical Properties of Silver Nanoparticles and Dye

The optical property of synthesized silver nanoparticles was characterized by UV-Vis spectroscopy and high resolution-transmission electron microscopy (HR-TEM). The absorption spectra of the synthesized silver nanoparticles are shown in Figure 3(a). The absorption band at about 400 nm is apparently due to the surface plasmon resonance (SPR) band of the Ag nanoparticles, and so, it

confirms the presence of the silver nanoparticles (AgNPs). The SPR results from the interaction of free electrons and electromagnetic radiation [19] reported that rhodamine 6G dyes can form dimers on the AgNPs surface which is related to localized surface plasmon resonance. This phenomenon enhances the absorption coefficients of the dye and optical absorption, which results in an increase in the efficiency of the solar cell [20] [21]. The AgNPsas well as the AgNPs-infused TiO_2 were characterized by transmission electron microscopy (TEM). The TEM allows for the visualization of the individual nanoparticles. The TEM images of the AgNPs with TiO_2 showed a close interaction of the AgNPs with TiO_2. The sizes of the AgNPs and titanium dioxide were similar, which accounts for the excellent interaction between the nanoparticles. The energy disperses X-ray spectrometry of the sample confirmed the presence of copper (Cu), carbon (C), and silver (Ag). The high percentage of copper in the spectrum is due to the copper TEM grid used for mounting the AgNPs sample. The carbon signal should come from the carbon-supporting film on the copper grid. The images of the analysis are displayed in **Figure 2**.

The optical property of rhodamine derivative **RdS1** was investigated using UV/Vis absorption and fluorescence spectroscopy. The dye solution showed no absorption above 400 nm, as shown in **Figure 3(b)**, which is typical for the most prominent ring-closed form of rhodamine derivatives [22]. The UV/Vis spectrum of **RdS1** was recorded in buffer at 25˚C and showed an absorption maximum at λ = 305 nm, which is attributed to the intramolecular π-π* charge transfer transition. Upon addition of copper(II) ion, the absorption peak at 300 nm decreased, and a new absorption band appeared at 525 nm, which can be attributed to the delocalized xanthene moiety of rhodamine and coordination of copper ion, as shown in **Figure 3(c)**. As demonstrated in **Scheme 2**, a monomeric system forms a 1:1 complex. The dye **RdS1** exhibited similar fluorescence spectroscopic properties upon binding with Cu^{2+}. As shown in **Figure 3(d)**, the fluorescence emission for **RdS1** appeared at 560 nm and as well as significant fluorescence intensity enhancement with 5 equivalents of Cu^{2+} ions.

3.2. Photovoltaic Performance of the DSSCs

The current-voltage (I-V) characteristics were measured to study the photoelectric performance of both the bare and plasmonic silver nanoparticles (AgNPs) incorporated dye-sensitized solar cells (DSSCs). The photovoltaic performances of the cells were determined via the measurements of maximum voltage (V_{max}), maximum current (I_{max}), open-circuit voltage (Voc), short-circuit current (Isc), fill factor (FF), and the power conversion efficiency (η) of the cell. By measuring the current and voltage of the constructed device, it was possible to determine the solar-to-electric power efficiency of the dye-sensitized solar cells [23]. The dye-sensitized solar cell device efficiency was calculated from **Figure 4** using the equation, where P_{max} and P_{in} denote the maximum output power and intensity of the incident light, respectively.

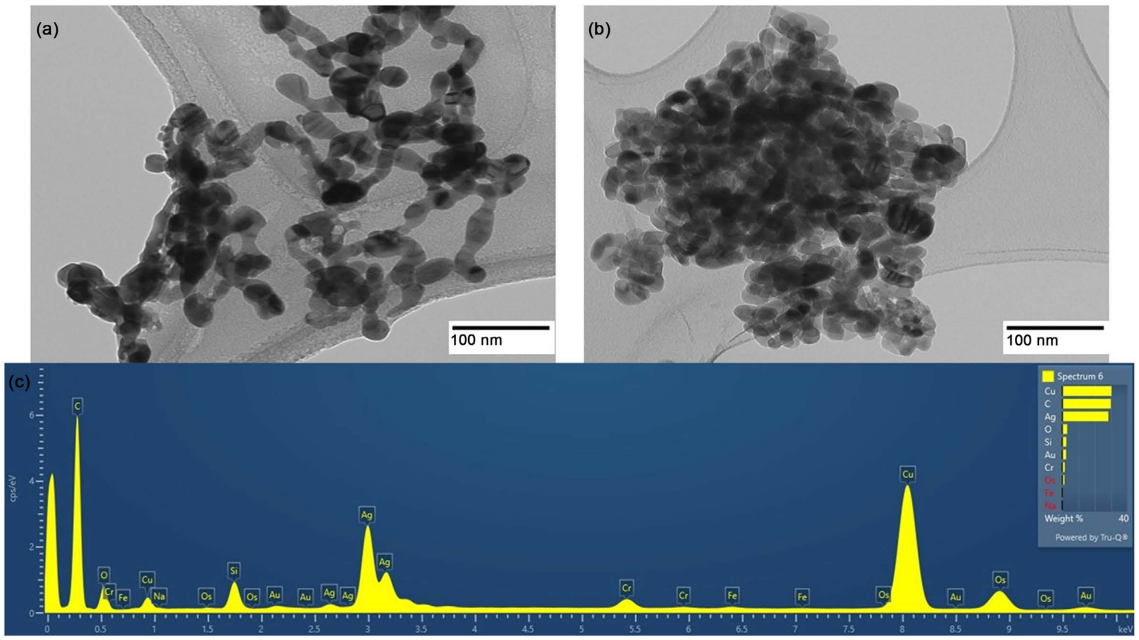

Figure 2. Transmission electron microscope images of silver nanoparticles (AgNPs) (a); AgNPs along with titanium dioxide nanoparticles (b); and energy-dispersive X-ray spectrometry analysis of AgNPs (c).

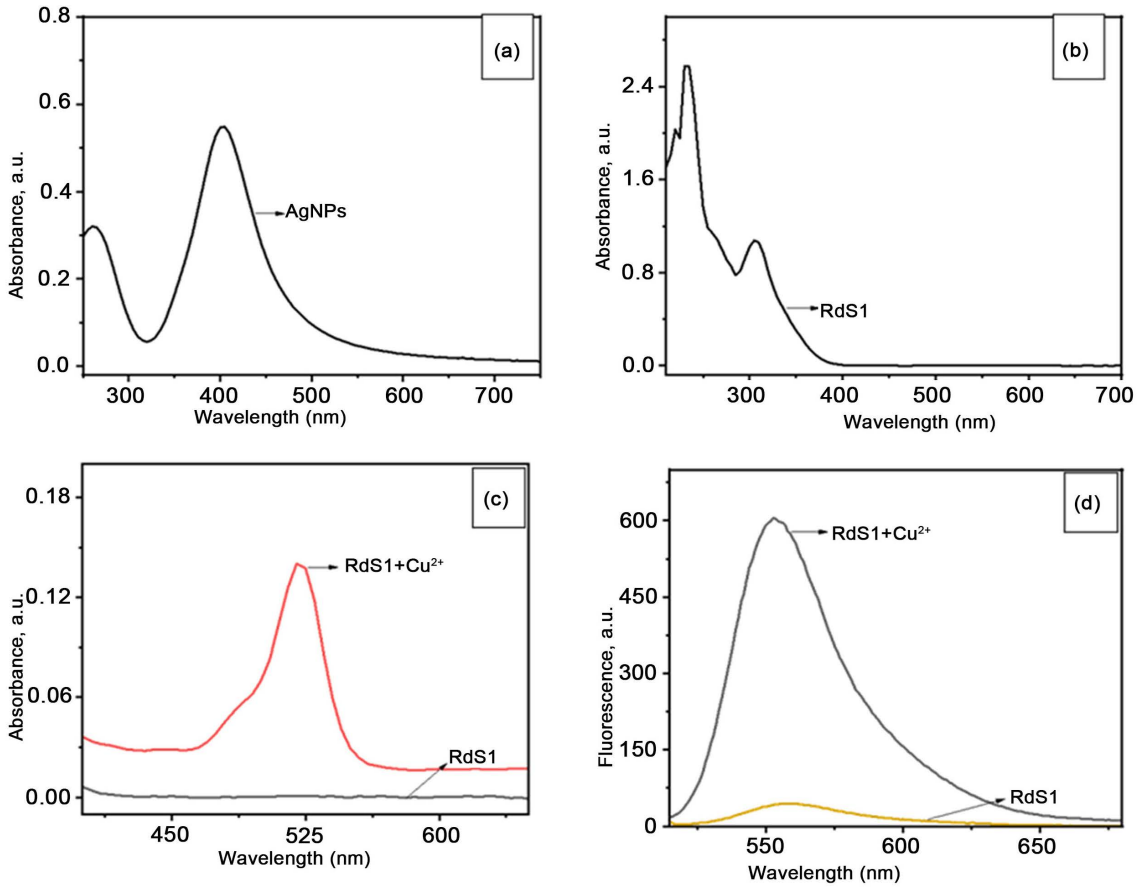

Figure 3. (a) Absorption spectra of Silver Nanoparticles (AgNPs); (b) UV/Vis absorption spectra of free dye **RdS1**, (c) UV/V is absorption spectra of **RdS1-Cu²⁺**; (d) Fluorescence emission spectra of **RdS1-Cu²⁺** in CH_3CN/H_2O (9:1 v/v) buffer solution (λ_{max} = 490 nm).

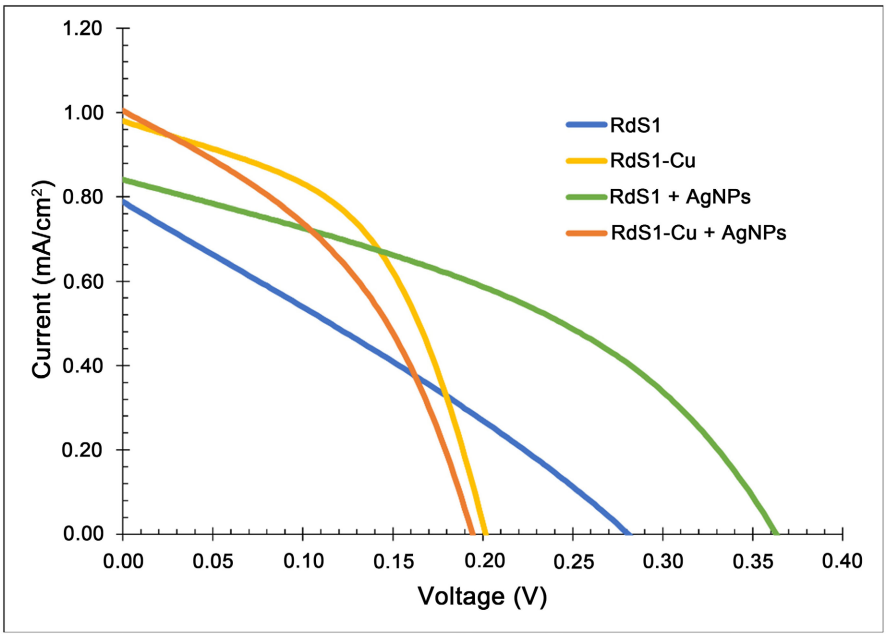

Figure 4. Current-voltage characteristics of the **RdS1** dye-sensitized solar cell measured under air-mass 1.5 global (AM 1.5 G) illumination having an irradiance of 100 mW/cm^2.

$$\eta(\%) = \frac{P_{\max}}{P_{in}} = (Voc * Isc * FF)/P_{in}$$

The solar-to-electric power conversion efficiency of the rhodamine dye-fabricated device was compared to the efficiencies of rhodamine-fabricated devices with silver nanoparticles incorporated DSSCs. Table 1 and Figure 4 show the current-voltage curves of the free rhodamine dye (**RdS1**), rhodamine-copper(II) complex (**RdS1-Cu^{2+}**), rhodamine with AgNPs (**RdS1 + AgNPs**), rhodamine-copper(II) complex with AgNPs (**RdS1-Cu^{2+} + AgNPs**). An increase in electric power efficiency was observed after the rhodamine dye **RdS1** was made to interact with AgNPs. The efficiency of the device with **RdS1** alone was 0.06% but increased to 0.17% after the addition of AgNPs. However, the solar-to-electric power efficiency of the device decreased to 0.08% with the introduction of AgNPs to the dye-copper(II) complex. Thus, the introduction of silver nanoparticles enhanced the light absorption abilities of the dye which consequently led to an increase in the efficiencies of dye-sensitized solar cells. The enhanced photovoltaic performance could be attributed to the plasmonic effect of the silver nanoparticles that result in a swift transfer of an electron from the AgNPs to the TiO_2 [24].

3.3. Electrochemical Impedance Measurements

The interfacial charge mechanisms of the DSSCs were addressed using electrochemical impedance spectroscopy (EIS). Impedance measurements were carried out on the fabricated DSSCs at frequencies between 1 Hz and 10^6 Hz under 100 mW/cm^2 illumination. Figure 5(a) shows the EIS-Nyquist plots of fabricated DSSCs. The semicircle in the high-frequency region corresponds to charge

Table 1. Photovoltaic performance of DSSCs with and without silver nanoparticles (AgNPs).

	V_{max} (V)	I_{max} (mA/cm²)	*Voc* (V)	*Isc* (mA/cm²)	Fill Factor	Efficiency (%)
RdS1	0.15	0.4	0.28	0.79	0.28	0.06
RdS1-Cu^{2+}	0.14	0.71	0.20	0.98	0.49	0.10
RdS1 + AgNPs	0.24	0.52	0.36	0.84	0.40	0.17
RdS1-Cu^{2+} + AgNPS	0.13	0.63	0.20	1.02	0.40	0.08

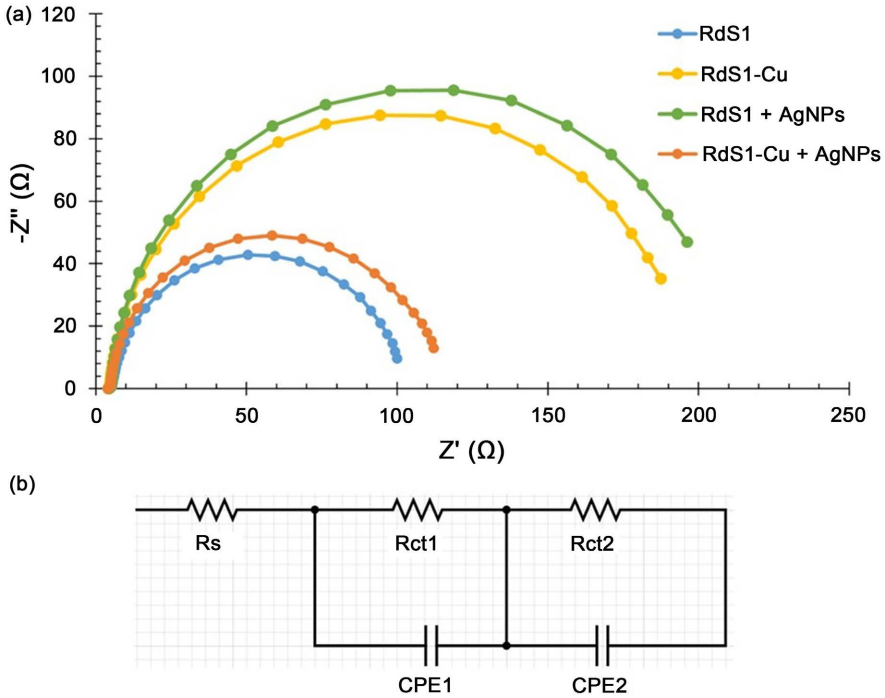

Figure 5. (a) Nyquist plot of the **RdS1** dye-sensitized solar cell measured under air-mass 1.5 global (AM 1.5 G) illumination having an irradiance of 100 mW/cm²; (b) Equivalent circuit model for EIS studies.

transport resistance (R_{ct1}) at the I^-/I_3^- graphite interface, and semicircle in the middle-frequency region is attributed to charge transport resistance (R_{ct2}) at the TiO_2/**RdS1** I^-/I_3^- interface. An equivalent circuit model of the EIS studies is shown in Figure 5(b). Faster electron transfer rates are associated with smaller resistances, which then result in improved efficiency of the DSSC. Conversely, larger resistances hinder the flow of electrons, thus reducing the performance of the DSSC [25]. From the Bode plots of Figure 6, the electron lifetimes (τ) of the DSSCs created were assessed. The electron lifetimes are inversely proportional to the peak frequency, as shown in the formula. The formula $\tau = 1/(2\pi f)$, where f is the peak frequency associated with the charge transfer and recombination kinetics at the sensitizer adsorbed photoanode/electrolyte interface, the lifetimes (τ) of **RdS1**, **RdS1-Cu^{2+}**, **RdS1 + AgNPs**, and **RdS1-Cu^{2+} + AgNPs** were calculated to be 3.19, 4.00, 5.00, and 2.51 ms respectively. The fabricated DSSC with **RdS1**

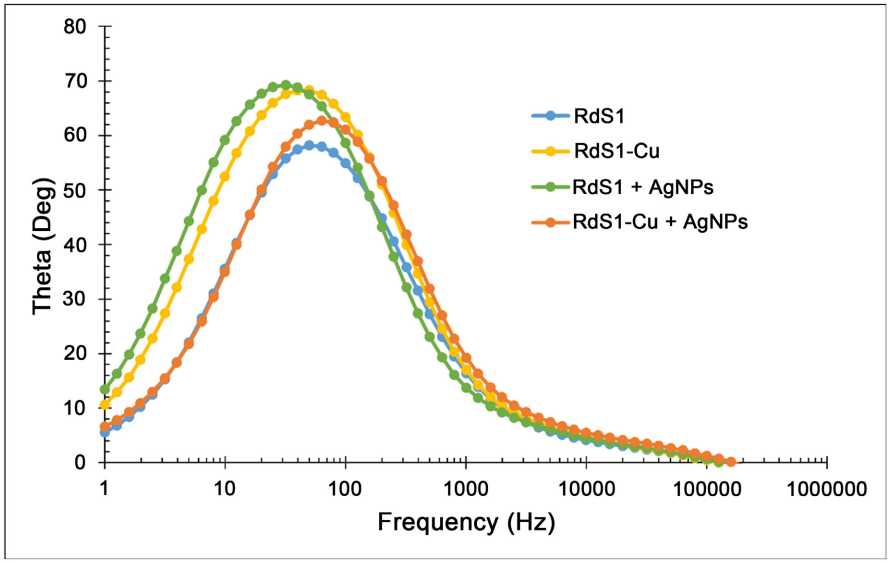

Figure 6. Bode plot of the RdS1dye-sensitized solar cell measured under air-mass 1.5 global (AM 1.5 G) illumination having an irradiance of 100 mW/cm^2.

Table 2. Peak frequency and lifetimes of the fabricated DSSCs.

	f_{max} (Hz)	τ (ms)	*Efficiency* (%)
RdS1	49.86	3.19	0.06
RdS1-Cu^{2+}	39.72	4.00	0.10
RdS1 + AgNPs	31.88	5.00	0.17
RdS1-Cu^{2+} + AgNPs	63.34	2.51	0.08

+ **AgNPs** having a higher electron lifetime compared to the DSSC devices agrees with the I-V measurements of the open-circuit voltage (V_{oc}) of the solar cells, which leads to the higher efficiency of the dye-sensitized solar cell. The peak frequency and lifetime of each fabricated DSSCs is summarized in Table 2.

4. Conclusion

In summary, Ag infused TiO_2 nanoparticles were prepared by sodium borohydride assisted simple reduction method. Through current-voltage (I-V) measurements, it was determined that the solar-to-electric power efficiency of solar cells sensitized with AgNPs infused in TiO_2 lattice was higher than the efficiency of devices without AgNPs. Electrochemical impedance (EIS) measurement reveals more efficient charge transportation and reduced recombination with AgNPs infusedTiO_2 based devices compared to bare TiO_2 based devices. The enhanced performance of the dye sensitized solar cell could be attributed to the plasmonic effect of the AgNPs. The study shows that the plasmonic nanoparticles can serve as an efficient material for future use in DSSCs.

Credit authorship Contribution Statement

Bandana Ranamagar: Conceptualization, Methodology, Investigation. **Isaac**

Abiye: Conceptualization, Methodology, Investigation, Data curation, review & editing. **Himsheela Karki:** Investigation. **Yucheng Lan:** Resources, Formal analysis, Data curation. **Fasil Abebe:** Conceptualization, Methodology, Investigation, Data curation, Writing-original draft.

Declaration of Competing Interest

The authors declare that they have no known competing financial interests or personal relationships that could have appeared to influence the work reported in this paper.

Data Availability

Data will be made available on request.

Acknowledgements

This research was supported by the National Science Foundation's Division of Chemistry under grant [2100629] and the National Institute of General Medical Sciences under [SC2GM125512] grants awarded to Morgan State University. TEM work was supported by the National Institute on Minority Health and Health Disparities under grant [5U54MD013376] and the National Institute of General Medical Sciences under [5UL1GM118973].

Conflicts of Interest

The authors declare no conflicts of interest regarding the publication of this paper.

References

[1] Roslan, N., Yaacob, M.E., Radzi, M.A.M., Hashimota, Y., Jamaludin, D. and Chen, G. (2018) Dye Sensitized Solar Cell (DSSC) Greenhouse Shading: New Insights for Solar Radiation Manipulation. *Renewable and Sustainable Energy Reviews*, **92**, 171-186. https://doi.org/10.1016/j.rser.2018.04.095

[2] Kuppu, S.V., Mohandoss, S., Murugesan, B., Venkatesan, S., Marimuthu, S., Chokalingam, S., Jeyaraman, A.R., Ahmed, N., Thambusamy, S. and Lee, Y.R. (2023) Development of Photo-Anode Materials for Dye Sensitized Solar Cell Using Natural Sensitized of Portulaca Grandiflora Flower-Soaked Titania Nanocrystalline and Nanofiber. *Chemical Physical Letters*, **812**, Article ID: 140271. https://doi.org/10.1016/j.cplett.2022.140271

[3] Kannan, U.M., Giribabu, L. and Narayana Jammalamadaka, S. (2019) Demagnetization Field Driven Charge Transport in a TiO_2 Based Dye Sensitized Solar Cell. *Solar Energy*, **187**, 281-289. https://doi.org/10.1016/j.solener.2019.05.029

[4] Ahmed, S.H.A., Al-Ahmed, A., Hakeem, A.S., Alshahrani, T., Mohmood, Q., Mehmood, U., Qayyum, H.A., Younas, M., Illyas, M., Dafalla, H., Jawaid, R., Laref, A. and Yago, A.J. (2021) Enhancing the Performance of Dye-Sensitized Solar Cell Using Nano-Sized Erbium Oxide on Titanium Oxide Photoanode by Impregnation Route. *Journal of Photochemistry and Photobiology*, **7**, Article ID: 100047. https://doi.org/10.1016/j.jpap.2021.100047

[5] Tontapha, S., Uppachai, P. and Amornkitbamrung, V. (2021) Fabrication of Functional Materials for Dye-Sensitized Solar Cells. *Frontiers Energy Research*, **9**, Article ID: 641983. https://doi.org/10.3389/fenrg.2021.641983

[6] Aduroja, O., Jani, M., Ghann, W., Ahmed, S., Uddin, J. and Abebe, F. (2022) Synthesis, Characterization, and Studies on Photophysical Properties of Rhodamine Derivatives and Metal Complexes in Dye-Sensitized Solar Cells. *ACS Omega*, **7**, 14611-14621. https://doi.org/10.1021/acsomega.1c06772

[7] Ranamagar, B., Abiye, I. and Abebe, F. (2023) Dye-Sensitized Solar Cells on TiO_2 Photoelectrodes Sensitized with Rhodamine. *Materials Letters*, **336**, Article ID: 133887. https://doi.org/10.1016/j.matlet.2023.133887

[8] Hou, W. and Cronin, S.B. (2013) A Review of Surface Plasmon Resonance-Enhanced Photocatalysis. *Advanced Functional Materials*, **23**, 1612-1619. https://doi.org/10.1002/adfm.201202148

[9] Zhou, N., Lopez, V., Wang, Q., Polavarapu, L., Patonria-Santos, I. and Xu, Q.H. (2015) Plasmon-Enhanced Light Harvesting Applications in Enhanced Photocatalysis, Photodynamic Therapy and Photovoltaics. *RSC Advances*, **5**, 29076-29097. https://doi.org/10.1039/C5RA01819F

[10] Aduroja, O., Abiye, I., Fathima, A., Tadesse, S., Ozturk, B., Wachira, J. and Abebe, F. (2023) Microwave-Assisted Synthesis for a Highly Selective Rhodamine 6G-Derived Fluorescent Sensor and Bioimaging. *Inorganic Chemistry Communications*, **147**, Article ID: 110236. https://doi.org/10.1016/j.inoche.2022.110236

[11] Aduroja, O., Shaw, R. and Abebe, F. (2022) A Bis(rhodamine 6G)-Based Fluorescent Sensor for Hg^{2+}: Microwave-Assisted Synthesis, Photophysical Properties, and Computational Studies. *Research on Chemical Intermediates*, **48**, 1847-1861. https://doi.org/10.1007/s11164-022-04704-x

[12] Solomon, S.D., Bahadory, M., Jeyarajasingam, A.V., Rutkowsky, S.A., Boritz, C. and Mulfinger, L. (2007) Synthesis and Study of Silver Nanoparticles. *Journal of Chemical Education*, **84**, 322-335. https://doi.org/10.1021/ed084p322

[13] Song, D.H., Kim, H.Y., Kim, H.S., Suh, J.S., Jun, B.H. and Rho, W.Y. (2017) Preparation of Plasmonic Monolayer with Ag and Au Nanoparticles for Dye-Sensitized Solar Cells. *Chemical Physics Letters*, **687**, 152-157. https://doi.org/10.1016/j.cplett.2017.08.051

[14] Blake-Hedges, J.M., Greenspan, S.H., Mathew, J.A., McCarron, M.A., Mendonca, M.L. and Wustholz, K.L. (2015) Plasmon-Enhanced Fluorescence of Dyes on Silica-Coated Silver Nanoparticles: A Single-Nanoparticle Spectroscopy Study. *Chemical Physics Letters*, **635**, 328-333. https://doi.org/10.1016/j.cplett.2015.06.083

[15] Dhonde, M., Sahu, K., Murty, V.V.S., Nemala, S.S. and Bhargava, P. (2017) Surface Plasmon Resonance Effect of Cu Nanoparticles in a Dye Sensitized Solar Cell. *Electrochimica Acta*, **249**, 89-95. https://doi.org/10.1016/j.electacta.2017.07.187

[16] Isah, K.U., Jolayemi, B.J., Ahmadu, U. and Kimpa, M.I. (2016) Plasmonic Effect of Silver Nanoparticles Intercalated into Mesoporous Betalain-Sensitized-TiO_2 Film Electrodes on Photovoltaic Performance of Dye-Sensitized Solar Cells. *Materials for Renewable and Sustainable Energy*, **5**, Article No. 10. https://doi.org/10.1007/s40243-016-0075-z

[17] Saravanan, S., Kato, R., Balamurugan, M., Kaushik, S. and Soga, T. (2017) Efficiency Improvement in Dye Sensitized Solar Cells by the Plasmonic Effect of Green Synthesized Silver Nanoparticles. *Journal of Science: Advanced Materials and Devices*, **2**, 418-414. https://doi.org/10.1016/j.jsamd.2017.10.004

[18] Abebe, F., Gonzalez, J., Makins-Dennis, K. and Shaw, R. (2020) A New Bis(rhodamine)-

Based Colorimetric Chemosensor for Cu^{2+}. *Inorganic Chemistry Communications*, **120**, Article ID: 108154. https://doi.org/10.1016/j.inoche.2020.108154

[19] Deng, H. and Yu, H. (2019) Silver Nanoparticle Surface Enabled Self-Assembly of Organic Dye Molecules. *Materials*, **12**, 2592. https://doi.org/10.3390/ma12162592

[20] Schaadt, D.M., Feng, B. and Yu, E.T. (2005) Enhanced Semiconductor Optical Absorption via Surface Plasmon Excitation in Metal Nanoparticles. *Applied Physics Letters*, **86**, Article ID: 063106. https://doi.org/10.1063/1.1855423

[21] Mock, J.J., Barbic, M., Smith, D.R., Schultz, D.A. and Schultz, S. (2002) Shape Effects in Plasmon Resonance of Individual Colloidal Silver Nanoparticles. *The Journal of Chemical Physics*, **116**, 6755-6759. https://doi.org/10.1063/1.1462610

[22] Abebe, F., Perkins, P., Shaw, R. and Tadesse, S. (2020) A Rhodamine-Based Fluorescent Sensor for Selective Detection of Cu^{2+} in Aqueous Media: Synthesis and Spectroscopic Properties. *Journal of Molecular Structure*, **1205**, Article ID: 127594. https://doi.org/10.1016/j.molstruc.2019.127594

[23] Chatterjee, S. (2018) Performance of Dye-Sensitized Solar Cells (DSSCs) Fabricated with Zinc Oxide (ZnO) Nanopowders and Nanorods. *Journal of Materials Engineering and Performance*, **27**, 2713-2718. https://doi.org/10.1007/s11665-018-3285-y

[24] Garmaroudi, Z.A. and Mohammadi, M.R. (2016) Plasmonic Effects of Infiltrated Silver Nanoparticles inside TiO_2 Film: Enhanced Photovoltaic Performance in DSSCs. *Journal of the American Ceramic Society*, **99**, 167-173. https://doi.org/10.1111/jace.13923

[25] Adhikari, S.G., Shamsaldeen, A. and Andersson, G.G. (2019) The Effect of $TiCl_4$ Treatment on the Performance of Dye-Sensitized Solar Cells. *The Journal of Chemical Physics*, **151**, Article ID: 164704. https://doi.org/10.1063/1.5125996